Supplement of Atmos. Chem. Phys., 25, 9275–9294, 2025
https://doi.org/10.5194/acp-25-9275-2025-supplement

Atmospheric Chemistry and Physics
Open Access
EGU

Supplement of

Photochemical aging of aviation emissions: transformation of chemical and physical properties of exhaust emissions from a laboratory-scale jet engine combustion chamber

Anni Hartikainen et al.

Correspondence to: Anni Hartikainen (anni.hartikainen@uef.fi) and Olli Sippula (olli.sippula@uef.fi)

Section 1. Offline chemical analyses

Section 1.1. GC×GC MS analyses

The GC×GC measurements were carried out on a Pegasus® GC-HRT 4D (LECO, St. Joeseph, USA) in combination with an OPTIC-4 GC inlet system (GL Sciences, Netherlands) using Helium as a carrier gas. For the measurements, a circular filter punch (diameter 3 mm) equal to 700 l of sampling volume was introduced into the OPTIC-4. For the fuel measurement, 1 µL of diluted jet fuel (DCM, 1:100 v/v) was applied to a desorbed filter punch. After 2 min of inlet purging (flow 0.1 mL min^{-1}, split flow 100 mL min^{-1}), a thermal desorption temperature gradient of 2 K s^{-1} was applied from 50 °C to 350 °C (flow 2 mL min^{-1}, splitless). After thermal desorption, the flow and split flow were set to 1 mL min^{-1} and 20 mL min^{-1}, respectively.

For the separation, a 60 m BPX5 (0.25 mm internal diameter, 0.25 µm film thickness) column in the 1st dimension and 1.5 m BPX50 (0.1 mm internal diameter, 0.1 µm film thickness) in the 2nd dimension was used. The initial primary GC oven temperature of 50 °C was held for 10 min and then ramped at 2 K min^{-1} to 345 °C which was held for 20 min. The secondary oven temperature offset was +5 °C to the primary oven and the modulator temperature offset was +15 °C to the secondary oven temperature. The modulation time was 3 s.

Ionization of the eluted compounds was performed by electron ionization with 70 eV at 250 °C. The obtained ions were acquired between *m/z* 40 to 500 in "high-resolution-mode" with an acquisition rate of 120 Hz. Perfluorotributylamine (PFTBA) was continuously added to the MS source as internal standard for mass calibration. Calibration and processing of acquired mass spectra was performed with the ChromaTOF HRT software (v5.10, LECO, St. Joe, USA).

Section 1.2. Gas phase analyses.

Adsorber tubes with three sublayers of GCB (Graphitized Carbon Black) sorbents were used for trapping gas-phase organics of different volatilities (Table S1). Adsorber tubes were conditioned under a protective nitrogen atmosphere at 350 °C for 1 h 30 min for conditioning. During sampling, a stainless-steel filter holder assembly was positioned between an empty glass tube upstream and the adsorber tube downstream to install a quartz fibre filter (QFF) in front of the adsorber tubes to remove particle fractions (Mason et al., 2020). These 13 mm pre-filters (precipitation area diameter of 10mm) had been punched from baked 47 mm QFF (Whatman QM-A, cytiva). Gillian GilAir Plus sampling pumps (Gilian, USA) were used for sampling for 240 min at a flow rate of 0.5 l min^{-1} accounting for a total volume of 120 l.

The offline analysis of gas phase samples was performed on the GCMS-QP2010 Ultra (Shimadzu, Japan) equipped with the thermal desorber unit (TD-20, Shimadzu). Thermal desorption occurred at 340 °C for 45 min. Extracted compounds were first concentrated at 5 °C on a Tenax TD trap, then re-desorbed at 300 °C for 30 min, after which they were transferred to the GC column at a split ratio of 50.

The separation took place on a VF-xMS, high-arylene-modified phase column (30 m + 5 m pre-column, 0.25 mm ø x 0.25 µm t, Agilent Varian, USA) at a column flow of 1.62 mL min^{-1}. GC oven temperature was 60 °C for a hold time of 6 min and then increased to a final temperature of 300°C at a rate of 5 °C min^{-1}. The MS was operated with ion source temperature of 230 °C and interface temperature of 250 °C in scan mode in the m/z range of 30 to 500. An isotope-labeled standard mixture was applied on the adsorber tubes prior to analysis and equivalent target compounds and similar target groups were quantified according to respective standard compounds as documented in Table S3. GCMSsolution Ver.2 software was used for peak identification and quantification.

Section 2. Conditions in the oxidation flow reactor

The external OH reactivity (OHR_{ext}) of the sampled exhaust was estimated based on the concentrations of CO, NO, NO_2, and THC_{FID} (as ppm propane) assuming reaction rates of 2.41×10^{-13}, 1×10^{-11}, 1.06×10^{-11}, and 1×10^{-12} cm^3 $molecules^{-1}$ s^{-1}, respectively. OHR_{ext} in the undiluted sample was approximately 14 000 s^{-1}, with 35 %, 45 %, and 20 % of the total caused by CO, THC, and NO_x, respectively. The OHR_{ext} was moderated by sample dilution, leading to OHR_{ext}s of 280 s^{-1} or 70 s^{-1} for the DR 50 and DR 200 experiments, respectively.

The particulate condensation sinks (CS_{PM}, Table S3) in the PEAR were estimated based on the size distributions measured by SMPS for fresh and aged exhaust downstream the PEAR (Hartikainen et al., 2020). LVOC fates were estimated as in Hartikainen et al., (2020) with the method based on Palm et al., (2016). Lifetime due to condensation to particles was estimated as 1/CS. LVOC partitioning onto particles was by far the major LVOC fate compared to reactions with OH (Supp. Table S2) or loss to walls (constant LVOC lifetime of 603 s). The photolysis rate in the PEAR for the varying lamp settings was estimated based on the known lamp power, lamp efficiency (30 %) and internal surface area (0.47 m^2) (Ihalainen et al., 2019), and the as ratio in exposure to photolysis exposure to OH exposure was calculated based on the known lamp settings and the OH exposure determined by butanol-d9 measurements.

Figures

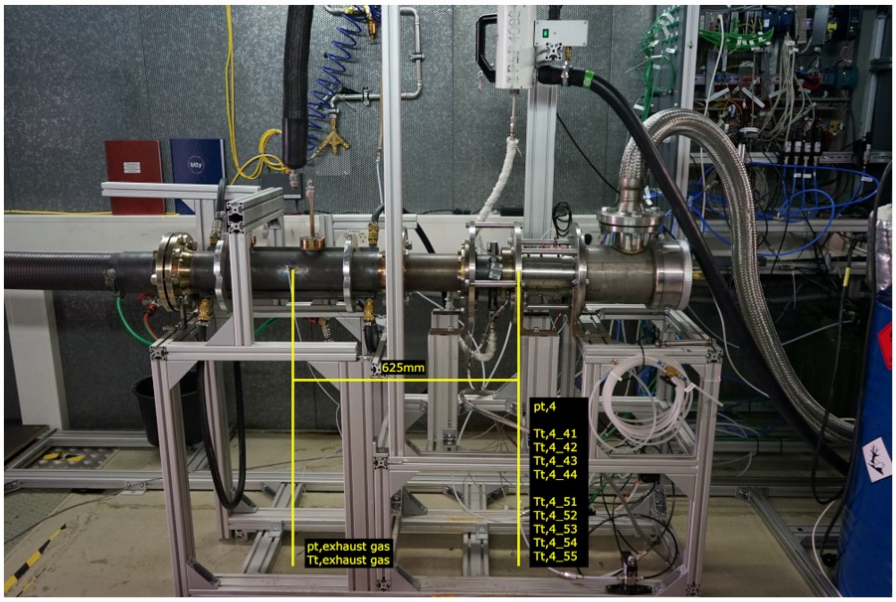

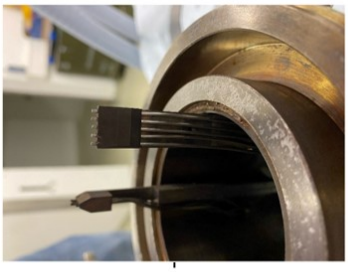

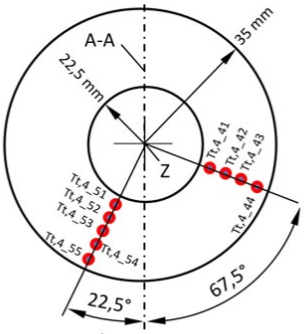

	Mass flow		Temperature											Pressure		
	$\dot{m}_{Fuel}$	$\dot{m}_{Air}$	Total inlet	Exhaust gas	Tt,4_41	Tt,4_42	Tt,4_43	Tt,4_44	Tt,4_51	Tt,4_52	Tt,4_53	Tt,4_54	Tt,4_55	Total inlet	Exhaust gas	pt,4
Unit	[g s^{-1}]	[g s^{-1}]	[°C]	[°C]	[°C]	[°C]	[°C]	[°C]	[°C]	[°C]	[°C]	[°C]	[°C]	[bar]	[bar]	[bar]
Mean	1.3	111	24.1	380	557	526	474	405	366	368	374	306	199	1.32	1.08	1.28
Std	0.01	0.53	0.4	5.1	9.6	15.4	44.1	58.2	15.1	11.3	10.9	17.2	26.7	0.02	0.01	0.01

Figure S1. The setup of the small-scale jet engine and its operation conditions presented as means and standard deviations of the means of eight operation days.

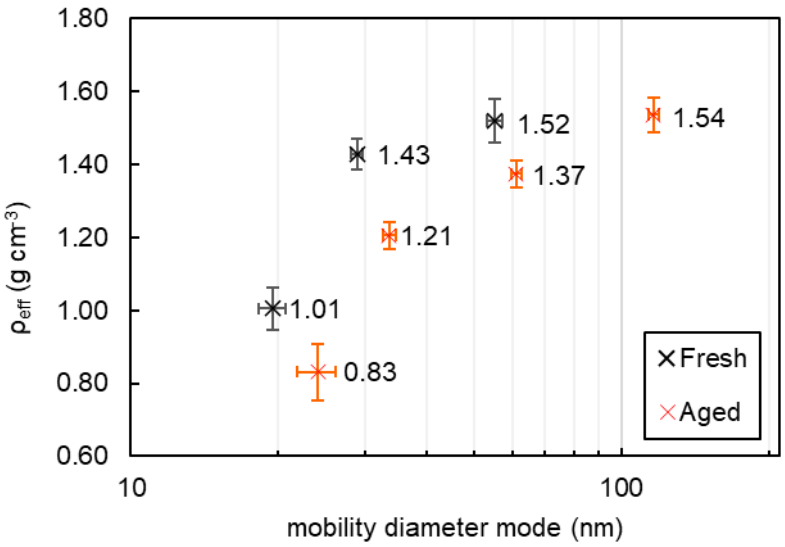

60 **Figure S2. Particle effective densities measured by the AAC-SMPS as a function of mobility diameter mode. The vertical error bars illustrate temporal variation in the densities as standard deviation during the measurements. The horizontal error bars indicate the standard deviation in the mobility diameter mode for each aerodynamic mode setpoint of the AAC (20, 40, 80, and 160 nm).**

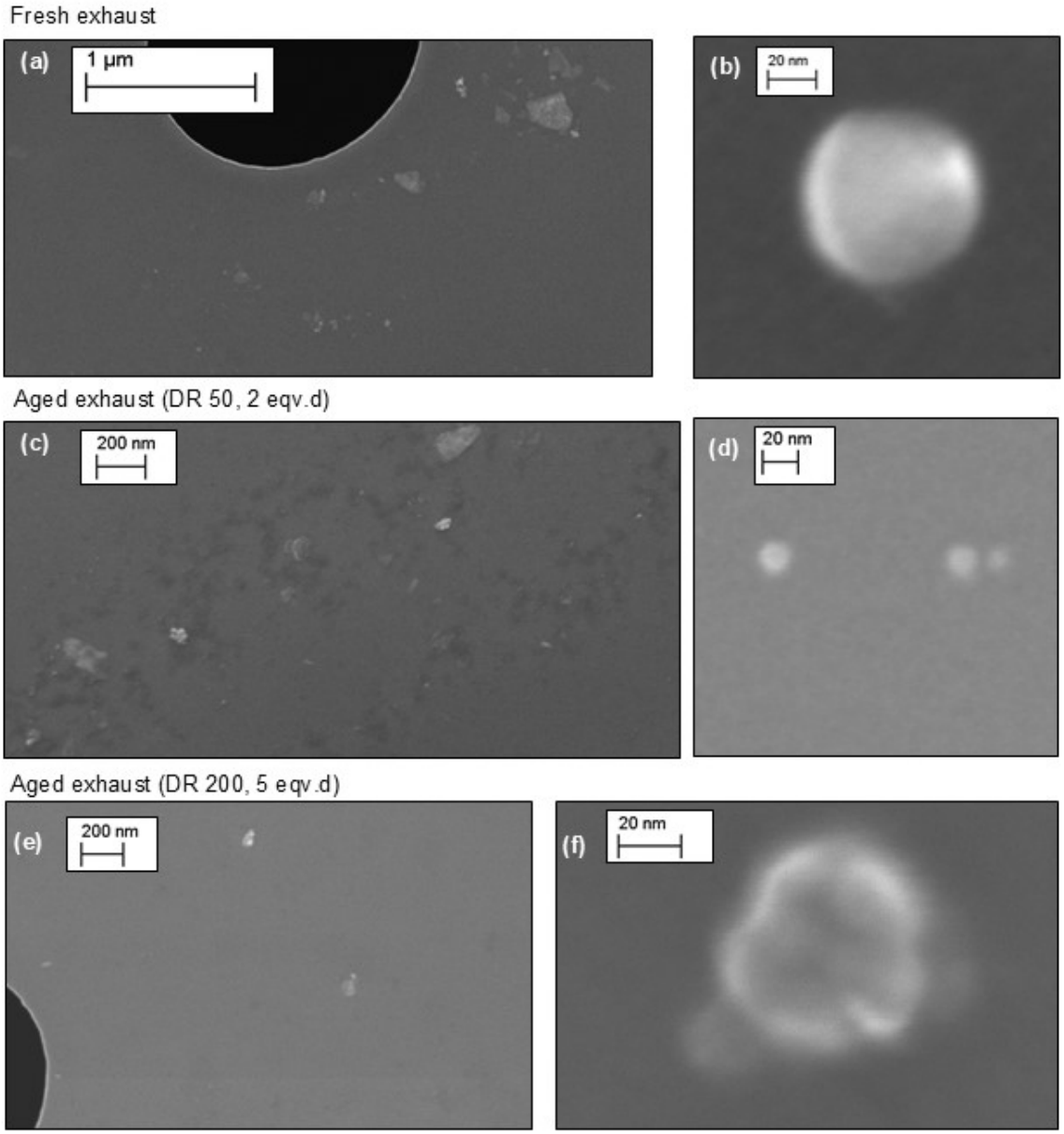

Figure S3. Scanning electron micrographs illustrating the morphology of the exhaust particles in the fresh (a-b) and aged emissions (c-d: photochemical age 2 eqv.d, dilution ratio 50; e-f: photochemical age 5 eqv.d, dilution ratio 200). The large black areas in A and E are holes in the grids. Note that no implications on average particle size are to be driven based on these images of single particles.

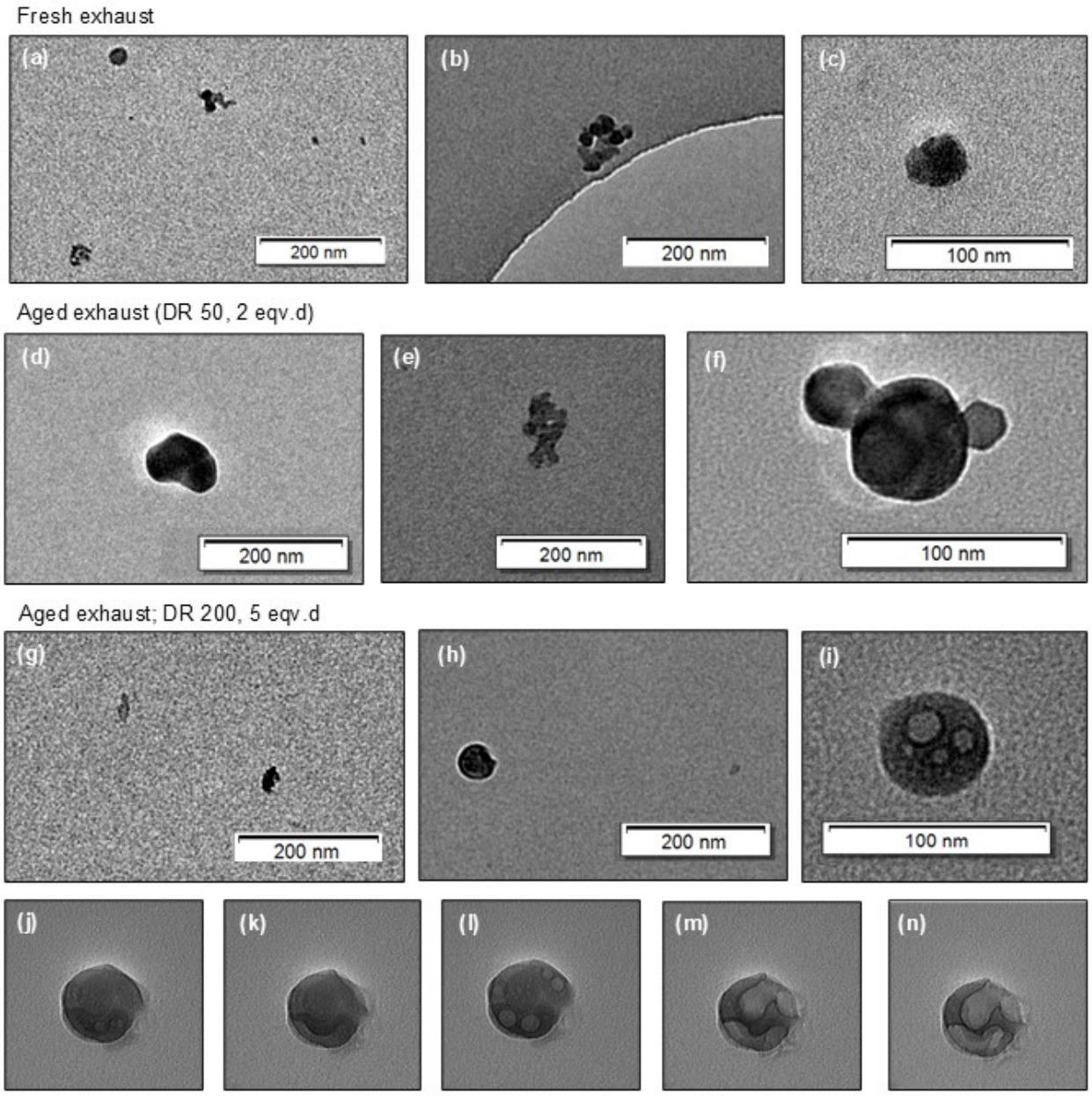

70 **Figure S4. Transmission electron micrographs illustrating the morphology of the non-volatile exhaust particles in the fresh (a-c) and aged emissions (d-f: photochemical age 2 eqv.d, dilution ratio 50; g-n: photochemical age 5 eqv.d, dilution ratio 200). Micrographs in j-n illustrate the evaporation of a single particle (original diameter approx. 80 nm) when focusing the electron beam. Note that no implications on average particle size are to be driven based on these images of single particles.**

75

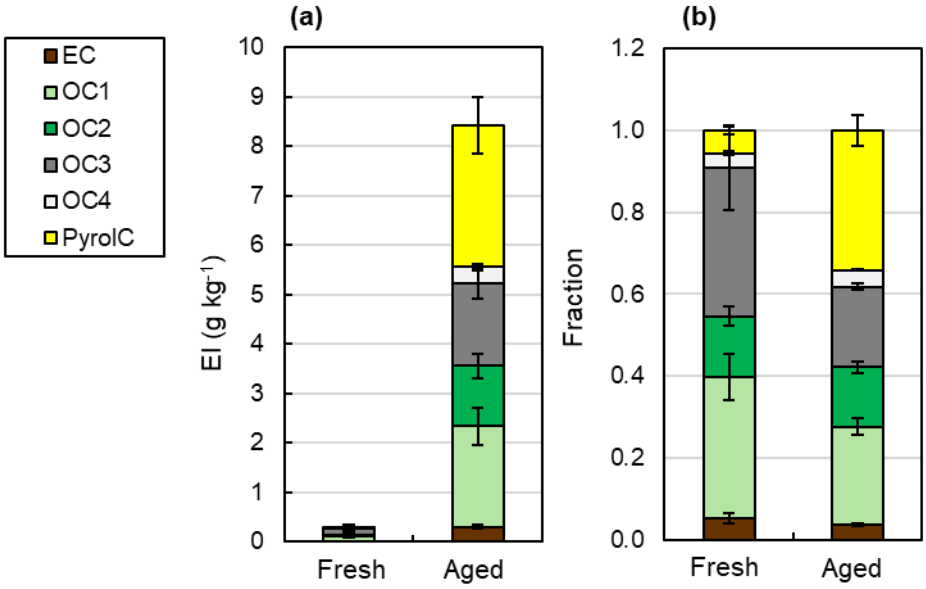

Figure S5. The absolute carbon EIs (a) and the relative fractions of the different volatility bins to the thermally derived carbon fractions to the total carbon content (b). Error bars in indicate the standard deviation of total EI (a) or fraction contribution (b) within filter samples collected from repetitions (n = 6 and 4 for fresh and aged exhausts, respectively).

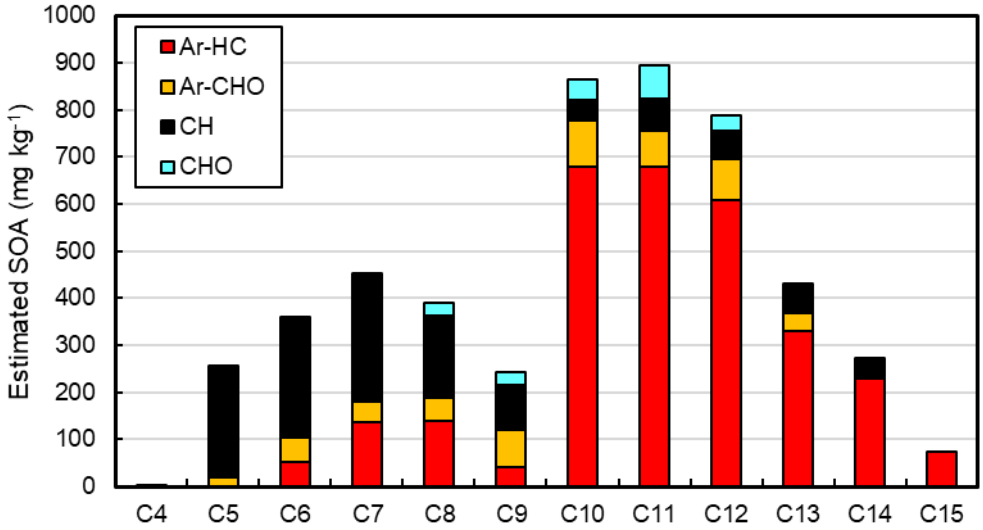

Figure S6. The bottom-up estimation of SOA production by compound group and number of carbon in the parent ion measured by PTR-ToF-MS.

Tables

Table S1. Composition of gas-phase adsorber tube containing three GCB layers separated by glass wool. Thermal desorption was carried out with reversed airflow.

Sampling order in direction of airflow	Sorbent	Weight (mg)
1	Carbotrap® B (20-40 mesh)	60
2	Carbotrap® Y (20-40 mesh)	60
3	Carbotrap® 569 (20-40 mesh)	60

Table S2. Oxidation flow reactor conditions in each run with the PEAR, and estimated lifetimes of LVOCs in the exhaust with respect to partitioning to particles (T_{aer}) or reactions with OH· (T_{OH}). * atmospheric equivalent days at [OH·] 1.5 ×10^6 cm^{-3}. ** at the PEAR exit.

Experiment run	OH_{exp}		$F_{254,\ exp}$ /OH_{exp}	CS_{PM} **	LVOC T_{aer}**	LVOC T_{OH}
	(10^{10} molec. cm^3 s^{-1})	(eqv.d*)	(cm s^{-1})	(s^{-1})	(ms)	(s)
DR50 experiments						
Run-2	~26	~2	1.6×10^6	470 ± 14	2 ± 0.1	130
Run-4	~26	~2	1.6×10^6	410 ± 11	2 ± 0.1	130
Run-7	~26	~2	1.6×10^6	420 ± 25	2 ± 0.2	130
Run-8	~26	~2	1.6×10^6	470 ± 11	2 ± 0.1	130
DR200 experiments						
Run-3	84	6.50	7.8×10^5	170 ± 6.3	6 ± 0.2	42
Run-3	41	3.20	6.0×10^5	170 ± 17	6 ± 0.7	85
Run-3	22	1.70	5.7×10^5	130 ± 6.2	7 ± 0.3	160
Run-3	8.1	0.60	7.6×10^5	85 ± 4.3	12 ± 0.6	430
Run-7	74	5.70	9.3×10^5	170 ± 4.5	6 ± 0.2	47
Run-7	4.9	0.38	1.3×10^6	95 ± 5.2	11 ± 0.6	720
Run-7	17	1.28	7.5×10^5	130 ± 8.3	7 ± 0.5	210
Run-8	84	6.49	8.1×10^5	190 ± 6.3	5 ± 0.2	42
Run-8	39	3.04	6.3×10^5	160 ± 20	6 ± 1	89
Run-8	21	1.64	2.9×10^5	77 ± 8.7	13 ± 1.6	160
Run-8	3.0	0.24	2.0×10^6	67 ± 0.4	15 ± 0.1	1150

Table S3. Internal standards used for quantification for GC-MS analyses.

Internal standard	Concentration (g L^{-1})	Targets
Toluene d8	0.2344	Ethylbenzene, Styrene
o-Xylene d10	0.0787	m-Xylene, o-Xylene
Naphthalene d8	0.0797	Indane, Indene, Naphthalene, 2-Methylnaphthalene, 1-Methylnaphthalene, 1,2 Dimethylnaphthalene
Biphenyl d10	0.0719	Biphenyl
Fluorene d10	0.0310	Fluorene
n-Dodecane d26	0.0693	Octadecane, Nonadecane, Decane, Undecane, Dodecane, Tridecane, Tetradecane
n-Hexadecane d34	0.0387	Pentadecane, Hexadecane, Heptadecane, Octadecane

Table S4. Ions measured by the PTR-ToF-MS: the applied reaction rates with H_3O^+ (k), the determined average emission indices in the fresh and aged exhausts at DR50, and the secondary organic aerosol yield applied for the bottom-up yield estimation. ks are interpolated to 136 Td from the values available in Cappellin et al., (2012). k of 2.00 × 10^{-9} cm^3 s^{-1} was otherwise assumed. SOA mass yields were estimated based on literature values similarly as in Hartikainen et al., (2024). std refers to standard deviation during the operation time in DR50 experiments.

m/z	ion formula	Group	DBE	k	EI, fresh		EI, aged		SOA yield
				(10^{-9} cm^3 s^{-1})	(mg kg_{fuel}^{-1})		(mg kg_{fuel}^{-1})		
					mean	std	mean	std	
41.04	(C3H4)H+	CH	2	1.61	1744	131	501	84	0 %
42.03	(C2H3N)H+	CHN	1.5	3.85	3	4	2	1	0 %
42.01	C2H2O+	CHO	2	2	15	2	10	1	0 %
42.04	C3H6+	CH	4	2	58	8	18	3	0 %
43.02	(C2H2O)H+	CHO	2.5	2	920	64	3329	306	0 %
43.05	(C3H6)H+	CH	1	1.62	914	95	340	66	0 %
45.03	(C2H4O)H+	CHO	1.5	3.04	2294	82	1603	197	0 %
47.01	(HCOOH)H+	CHO	2	1.91	540	51	2412	354	0 %
47.05	(C2H6O)H+	CHO	0.5	2.07	5	2	2	3	0 %
49.03	(CH4O2)H+	CHO	0	2	6	1	74	11	0 %
49.02	CH4S-H+	CHS	1	2	2	1	4	2	0 %
53.04	(C4H4)H+	CH	3	2	49	3	14	2	0 %
55.05	(C4H6)H+	CH	3.5	1.8	1419	142	469	93	0 %
55.02	(C3H2O)H+	CHO	2	2	66	9	85	8	0 %
57.03	(C3H4O)H+	CHO	2.5	3.04	607	27	258	35	0 %
57.07	(C4H8)H+	CH	1	1.8	1509	147	362	81	0 %
59.05	(C3H6O)H+	CHO	1.5	3.01	1249	56	1898	131	0 %
61.03	(C2H4O2)H+	CHO	2	2.01	921	45	4023	417	0 %
63.01	(CH2O3)H+	CHO	2.5	2	<1		51	11	0 %
65.02	(CH4O3)H+	CHO	1.5	2	2	1	38	5	0 %
67.06	(C5H6)H+	CH	3	1.83	210	13	65	11	0 %
69.03	(C4H4O)H+	CHO	3.5	2	126	6	70	8	0 %
69.07	(C5H8)H+	CH	2	2	968	93	268	61	26 %
71.01	(C3H2O2)H+	CHO	4	2	16	8	56	8	0 %
71.05	(C4H6O)H+	CHO	2.5	3.29	487	21	201	30	0 %
71.08	(C5H10)H+	CH	1	1.9	260	28	54	14	26 %
73.03	(C3H4O2)H+	CHO	3	2.55	319	12	290	27	0 %
73.06	(C4H8O)H+	CHO	1.5	2.99	375	20	489	48	0 %
75.04	(C3H6O2)H+	CHO	2	2.27	167	12	941	94	0 %
77.02	(C2H4O3)H+	CHO	2.5	2	10	3	379	99	0 %
79.05	(C6H6)H+	Ar-CH	4	1.93	258	18	119	20	37 %
81.03	(C5H4O)H+	Ar-CHO	4.5	2	27	6	11	2	30 %
81.07	(C6H8)H+	CH	3	2	476	39	129	25	26 %
83.01	(C4H2O2)H+	Ar-CHO	5	2	4	5	23	3	30 %
83.05	(C5H6O)H+	CHO	3.5	2	281	10	121	14	0 %
83.08	(C6H10)H+	CH	2	2	678	61	144	39	26 %
85.03	(C4H4O2)H+	CHO	4	2	196	11	242	33	0 %
85.06	(C5H8O)H+	CHO	2.5	2	390	17	304	40	0 %
85.1	(C6H12)H+	CH	1	2.02	133	15	29	9	26 %

87.04	(C4H6O2)H+	CHO	4.5	1.7	524	32	958	56	0 %
87.08	(C5H10O)H+	CHO	3	3.07	138	11	152	22	0 %
87.01	(C3H2O3)H+	CHO	1.5	2	3	8	18	14	0 %
89.02	(C3H4O3)H+	CHO	3.5	2	26	5	129	12	0 %
89.06	(C4H8O2)H+	CHO	2	4.18	47	4	209	25	0 %
90.02	(C2H3NO3)H+	CHNO	3	2	22	5	71	16	0 %
91.04	(C3H6O3)H+	CHO	4	2	5	17	58	13	0 %
91	(C2H2O4)H+	CHO	2.5	2	<1		6	5	0 %
91.05	(C7H6)H+	Ar-CH	5	2	131	18	26	5	37 %
93.07	(C7H8)H+	Ar-CH	3	2.08	320	31	58	13	37 %
93.04	(C6H4O)H+	Ar-CHO	5.5	2	2	7	4	2	30 %
93.02	(C2H4O4)H+	n.i.	4	2	<1		4	1	36 %
95.05	(C6H6O)H+	Ar-CHO	6	2.14	142	11	42	5	30 %
95.08	(C7H10)H+	CH	4.5	2	639	56	120	27	30 %
95.01	(C5H2O2)H+	Ar-CHO	3	2	1	4	4	5	26 %
97.03	(C5H4O2)H+	Ar-CHO	5	3.89	114	6	63	7	30 %
97.06	(C6H8O)H+	CHO	3.5	2	334	14	151	19	0 %
97.1	(C7H12)H+	CH	2	2.09	553	55	94	27	26 %
99.01	(C4H2O3)H+	Ar-CHO	5.5	2	554	34	603	96	30 %
99.04	(C5H6O2)H+	CHO	4	2	314	18	414	48	0 %
99.08	(C6H10O)H+	CHO	2.5	3.69	146	10	114	18	0 %
101.02	(C4H4O3)H+	CHO	4.5	2	25	28	380	73	0 %
101.06	(C5H8O2)H+	CHO	3	2.9	305	20	512	51	0 %
101.09	(C6H12O)H+	CHO	1.5	2.71	100	11	90	17	0 %
103.04	(C4H6O3)H+	CHO	3.5	2	37	7	136	19	0 %
103.07	(C5H10O2)H+	CHO	2	2	67	6	222	32	0 %
105.03	(C7H4O)H+	Ar-CHO	6.5	2	8	5	41	15	30 %
105.07	(C8H8)H+	Ar-CH	2.5	2.27	238	38	25	5	30 %
105.05	(C4H8O3)H+	n.i.	5	2	11	39	28	7	0 %
107.05	(C7H6O)H+	Ar-CHO	5.5	3.67	65	5	20	4	30 %
107.08	(C8H10)H+	Ar-CH	4	2.26	286	24	38	9	30 %
109.06	(C7H8O)H+	Ar-CHO	6	2.31	118	12	39	5	30 %
109.03	(C6H4O2)H+	Ar-CHO	4.5	1.99	37	4	75	8	35 %
109.1	(C8H12)H+	CH	3	2	528	50	85	21	26 %
111.04	(C6H6O2)H+	Ar-CHO	5	2	149	10	108	13	39 %
111.08	(C7H10O)H+	CHO	3.5	2	270	11	118	19	0 %
111.12	(C8H14)H+	CH	2	2	276	28	43	13	26 %
113.02	(C5H4O3)H+	Ar-CHO	5.5	2	111	13	208	14	30 %
113.06	(C6H8O2)H+	CHO	4	2	238	14	300	38	0 %
113.09	(C7H12O)H+	CHO	2.5	2	224	16	153	27	0 %
115.01	(C4H2O4)H+	Ar-CHO	6	2	7	7	22	4	30 %
115.04	(C5H6O3)H+	CHO	4.5	2	27	17	143	18	0 %
115.07	(C6H10O2)H+	CHO	3	2	267	16	478	52	0 %
115.11	(C7H14O)H+	CHO	1.5	2.78	95	13	81	17	0 %
117.02	(C4H4O4)H+	CHO	5	2	<1		11	3	0 %
117.05	(C5H8O3)H+	CHO	3.5	2	10	7	73	10	0 %
117.09	(C6H12O2)H+	CHO	6	2	56	8	127	21	6 %
117.07	(C9H8)H+	Ar-CH	2	2.42	32	4	<1		0 %
119.05	(C8H6O)H+	Ar-CHO	6.5	2	11	12	27	5	30 %

119.08	(C9H10)H+	Ar-CH	5	2	289	22	34	10	6 %
121.03	(C7H4O2)H+	Ar-CHO	7	2	1	5	7	3	30 %
121.06	(C8H8O)H+	Ar-CHO	5.5	3.28	113	13	38	7	30 %
121.1	(C9H12)H+	Ar-CH	4	2.4	464	48	38	11	6 %
123.04	(C7H6O2)H+	Ar-CHO	6	2.64	78	9	69	11	30 %
123.08	(C8H10O)H+	Ar-CHO	4.5	2	127	13	46	8	30 %
123.12	(C9H14)H+	CH	3	2	346	32	51	14	26 %
125.02	(C6H4O3)H+	Ar-CHO	6.5	2	74	13	51	8	30 %
125.06	(C7H8O2)H+	Ar-CHO	5	2	127	11	115	16	30 %
125.09	(C8H12O)H+	CHO	3.5	2	244	14	107	21	0 %
125.13	(C9H16)H+	CH	2	2	95	13	18	5	26 %
127.04	(C6H6O3)H+	Ar-CHO	5.5	2	46	10	105	12	30 %
127.07	(C7H10O2)H+	CHO	4	2	179	14	216	35	0 %
127.11	(C8H14O)H+	CHO	2.5	2	166	13	97	20	0 %
129.06	(C10H8)H+	Ar-CH	6	2.45	128	23	2	4	30 %
129.13	(C8H16O)H+	CHO	4.5	2.93	70	10	43	12	0 %
129.09	(C7H12O2)H+	CHO	7	2	321	42	331	50	73 %
129.02	(C5H4O4)H+	Ar-CHO	3	2	3	3	14	4	0 %
129.05	(C6H8O3)H+	CHO	1.5	2	7	12	143	19	0 %
131.03	(C5H6O4)H+	CHO	5	2	5	6	32	10	0 %
131.07	(C6H10O3)H+	CHO	7.5	2	8	22	46	8	0 %
131.1	(C7H14O2)H+	CHO	3.5	2	51	10	70	13	0 %
131.08	(C10H10)H+	n.i.	6	2	120	19	2	3	0 %
131.05	(C9H6O)H+	n.i.	2	2	17	6	1	3	0 %
133.03	(C8H4O2)H+	Ar-CHO	8	2	2	6	33	9	30 %
133.06	(C9H8O)H+	Ar-CHO	6.5	2	39	22	27	5	30 %
133.1	(C10H12)H+	Ar-CH	5	2	366	35	27	11	73 %
135.04	(C8H6O2)H+	Ar-CHO	7	2	69	11	60	12	30 %
135.08	(C9H10O)H+	Ar-CHO	5.5	2	208	32	53	11	30 %
135.11	(C10H14)H+	Ar-CH	4	2.5	572	64	32	10	73 %
137.06	(C8H8O2)H+	Ar-CHO	6	2	78	10	79	11	30 %
137.09	(C9H12O)H+	Ar-CHO	4.5	2	110	14	40	8	30 %
137.13	(C10H16)H+	CH	3	2.47	193	18	25	7	26 %
139.04	(C7H6O3)H+	Ar-CHO	6.5	2	51	11	59	17	30 %
139.07	(C8H10O2)H+	Ar-CHO	5	2	110	15	110	19	30 %
139.11	(C9H14O)H+	CHO	3.5	2	223	15	88	20	0 %
139.15	(C10H18)H+	n.i.	1	2	52	11	13	4	0 %
141.05	(C7H8O3)H+	Ar-CHO	7	2	40	11	101	15	30 %
141.09	(C8H12O2)H+	CHO	5.5	2	150	14	159	30	30 %
141.13	(C9H16O)H+	CHO	4	2	137	12	68	18	0 %
141.02	(C6H4O4)H+	Ar-CHO	2.5	2	3	3	24	6	0 %
143.1	(C8H14O2)H+	CHO	6	2	225	36	140	26	30 %
143.03	(C6H6O4)H+	Ar-CHO	4.5	2	<1		26	7	0 %
143.14	(C9H18O)H+	CHO	7	3.17	69	10	31	9	63 %
143.07	(C7H10O3)H+	CHO	3	2	27	82	131	19	0 %
143.08	(C11H10)H+	Ar-CH	1.5	2.7	343	48	5	6	0 %
145.05	(C6H8O4)H+	CHO	5	2	6	10	36	11	0 %
145.09	(C7H12O3)H+	CHO	7.5	2	16	43	27	6	0 %
145.12	(C8H16O2)H+	CHO	3.5	2	43	15	42	10	0 %

145.1	(C11H12)H+	Ar-CH	6	2	213	45	3	4	63 %
145.06	(C10H8O)H+	n.i.	2	2	32	12	3	5	0 %
147.04	(C9H6O2)H+	Ar-CHO	8	2	44	9	63	16	30 %
147.12	(C11H14)H+	Ar-CH	6.5	2	493	62	21	8	30 %
147.08	(C10H10O)H+	Ar-CHO	5	2	58	34	32	7	63 %
149.02	(C8H4O3)H+	Ar-CHO	8.5	2	263	37	392	77	30 %
149.06	(C9H8O2)H+	Ar-CHO	7	2	147	28	134	28	30 %
149.09	(C10H12O)H+	Ar-CHO	5.5	2	194	41	52	11	30 %
149.13	(C11H16)H+	Ar-CH	4	2	679	73	36	12	63 %
151.04	(C8H6O3)H+	Ar-CHO	7.5	2	18	5	19	4	30 %
151.07	(C9H10O2)H+	Ar-CHO	6	2	64	8	56	10	30 %
151.11	(C10H14O)H+	Ar-CHO	4.5	2	108	19	34	8	30 %
151.15	(C11H18)H+	CH	3	2	240	26	25	7	26 %
153.09	(C9H12O2)H+	Ar-CHO	6.5	2	101	19	97	20	30 %
153.13	(C10H16O)H+	CHO	5	2	209	21	72	19	30 %
153.16	(C11H20)H+	CH	3.5	2	45	9	9	4	30 %
153.05	(C8H8O3)H+	Ar-CHO	2	2	24	8	40	8	0 %
155.1	(C9H14O2)H+	CHO	7	4.93	47	5	34	8	30 %
155.03	(C7H6O4)H+	Ar-CHO	5.5	2	<1		16	5	30 %
155.14	(C10H18O)H+	CHO	4	2	139	16	56	16	0 %
155.07	(C8H10O3)H+	Ar-CHO	2.5	2	65	19	96	16	0 %
157.05	(C7H8O4)H+	Ar-CHO	6	2	12	7	48	10	30 %
157.08	(C8H12O3)H+	CHO	4.5	2	77	124	105	17	0 %
157.12	(C9H16O2)H+	CHO	7	2	237	44	115	29	0 %
157.16	(C10H20O)H+	CHO	3	3.03	83	12	35	12	0 %
157.1	(C12H12)H+	n.i.	1.5	2	566	111	5	11	0 %
159.08	(C11H10O)H+	n.i.	5	2	22	12	<1		0 %
159.06	(C7H10O4)H+	CHO	7.5	2	25	9	39	9	0 %
159.1	(C8H14O3)H+	n.i.	2	2	22	45	19	5	0 %
159.14	(C9H18O2)H+	CHO	1	2	46	14	23	7	0 %
159.11	(C12H14)H+	n.i.	2	2	196	46	6	5	0 %
161.06	(C10H8O2)H+	Ar-CHO	8	2	37	10	44	11	30 %
161.09	(C11H12O)H+	Ar-CHO	6.5	2	79	39	27	7	30 %
161.13	(C12H16)H+	Ar-CH	5	2	463	61	16	7	58 %
163.04	(C9H6O3)H+	Ar-CHO	8.5	2	166	44	267	57	30 %
163.07	(C10H10O2)H+	Ar-CHO	7	2	137	34	96	25	30 %
163.11	(C11H14O)H+	Ar-CHO	5.5	2	136	52	46	10	30 %
163.14	(C12H18)H+	Ar-CH	4	2	635	64	32	11	58 %
165.02	(C8H4O4)H+	Ar-CHO	9	2	6	4	8	2	30 %
165.05	(C9H8O3)H+	Ar-CHO	7.5	2	19	5	27	7	30 %
165.09	(C10H12O2)H+	Ar-CHO	6	2	48	10	42	9	30 %
165.13	(C11H16O)H+	Ar-CHO	4.5	2	119	24	34	9	30 %
165.16	(C12H20)H+	CH	3	2	251	31	20	7	26 %
167.1	(C10H14O2)H+	Ar-CHO	8	2	95	22	82	20	30 %
167.07	(C9H10O3)H+	Ar-CHO	6.5	2	25	9	39	9	30 %
167.14	(C11H18O)H+	CHO	5	2	217	24	63	17	30 %
167.03	(C8H6O4)H+	Ar-CHO	3.5	2	3	2	10	3	0 %
169.05	(C8H8O4)H+	Ar-CHO	7	2	3	4	20	5	30 %
169.08	(C9H12O3)H+	Ar-CHO	5.5	2	74	21	82	16	30 %

169.12	(C10H16O2)H+	CHO	4	2.86	118	15	62	16	0 %
169.16	(C11H20O)H+	CHO	2.5	2	153	19	52	17	0 %
171.06	(C8H10O4)H+	Ar-CHO	6	2	23	11	46	10	0 %
171.1	(C9H14O3)H+	CHO	4.5	4.72	12	22	33	7	0 %
171.13	(C10H18O2)H+	CHO	3	2	253	43	91	29	0 %
171.17	(C11H22O)H+	CHO	1.5	2	126	17	61	21	0 %
173.05	(C11H8O2)H+	Ar-CHO	9	2	10	4	17	5	30 %
173.09	(C8H12O4)H+	CHO	5	2	29	18	19	6	0 %
173.13	(C13H16)H+	Ar-CH	5	2	167	22	17	6	0 %
173.08	C8H12O4	n.i.	6	2	7	5	17	5	58 %
173.15	(C10H20O2)H+	n.i.	2	2	28	13	10	4	0 %
175.04	(C10H6O3)H+	Ar-CHO	9.5	2	5	4	13	3	30 %
175.07	(C11H10O2)H+	Ar-CHO	8	2	21	7	26	7	30 %
175.11	(C12H14O)H+	Ar-CHO	6.5	2	72	34	18	6	30 %
175.15	(C13H18)H+	Ar-CH	5	2	326	46	11	5	58 %
177.05	(C10H8O3)H+	Ar-CHO	8.5	2	61	31	102	23	30 %
177.09	(C11H12O2)H+	Ar-CHO	7	2	39	27	44	13	0 %
177.12	(C12H16O)H+	Ar-CHO	5.5	2	116	55	27	8	30 %
177.16	(C13H20)H+	Ar-CH	4	2	521	74	25	9	30 %
179.03	(C9H6O4)H+	Ar-CHO	9	2	3	2	10	3	30 %
179.07	(C10H10O3)H+	Ar-CHO	7.5	2	14	5	18	5	30 %
179.1	(C11H14O2)H+	Ar-CHO	6	2	40	11	34	8	30 %
179.14	(C12H18O)H+	Ar-CHO	4.5	2	119	27	29	9	30 %
179.18	(C13H22)H+	CH	3	2	253	36	17	5	26 %
181.04	(C9H8O4)H+	Ar-CHO	8	2	3	2	11	3	30 %
181.08	(C10H12O3)H+	Ar-CHO	6.5	2	19	9	36	9	30 %
181.12	(C11H16O2)H+	Ar-CHO	5	2	93	25	68	18	30 %
181.16	(C12H20O)H+	CHO	3.5	2	199	23	48	14	0 %
183.13	(C11H18O2)H+	CHO	7	2	152	24	71	21	30 %
183.17	(C12H22O)H+	CHO	5.5	2	155	20	44	14	30 %
183.1	(C10H14O3)H+	Ar-CHO	4	2	51	18	64	15	0 %
183.06	(C9H10O4)H+	Ar-CHO	2.5	2	5	4	22	6	0 %
185.08	(C9H12O4)H+	Ar-CHO	6	2	6	6	45	10	30 %
185.11	(C10H16O3)H+	CHO	4.5	3.82	40	16	32	7	0 %
185.15	(C11H20O2)H+	CHO	3	2	238	36	74	28	0 %
185.19	(C12H24O)H+	CHO	1.5	2	124	19	59	23	0 %
189.05	(C11H8O3)H+	Ar-CHO	9.5	2	3	3	14	4	30 %
189.16	(C14H20)H+	Ar-CH	5	2	188	27	6	4	30 %
191.07	(C11H10O3)H+	Ar-CHO	8.5	2	32	13	47	10	30 %
191.1	(C12H14O2)H+	Ar-CHO	7	2	50	15	25	8	30 %
191.14	(C13H18O)H+	Ar-CHO	5.5	2	67	36	17	6	30 %
191.18	(C14H22)H+	Ar-CH	4	2	318	45	15	6	58 %
193.04	(C10H8O4)H+	Ar-CHO	9	2	2	2	11	3	30 %
193.08	(C11H12O3)H+	Ar-CHO	7.5	2	8	4	14	4	30 %
193.12	(C12H16O2)H+	Ar-CHO	6	2	31	11	25	7	30 %
193.16	(C13H20O)H+	Ar-CHO	4.5	2	96	20	22	7	30 %
193.19	(C14H24)H+	CH	3	2	172	27	11	4	26 %
195.1	(C11H14O3)H+	Ar-CHO	6.5	2	15	8	34	9	30 %
195.13	(C12H18O2)H+	Ar-CHO	5	2	72	22	48	14	30 %

195.17	(C13H22O)H+	CHO	3.5	2	169	24	35	11	0 %
197.08	(C10H12O4)H+	Ar-CHO	7	2	5	4	24	6	30 %
197.11	(C11H16O3)H+	Ar-CHO	5.5	2	34	14	49	12	30 %
197.15	(C12H20O2)H+	CHO	4	2	117	24	46	16	0 %
197.19	(C13H24O)H+	CHO	2.5	2	148	22	33	12	0 %
199.1	(C10H14O4)H+	Ar-CHO	6	2	6	5	39	9	30 %
199.13	(C11H18O3)H+	CHO	4.5	2	35	22	41	10	0 %
199.17	(C12H22O2)H+	CHO	3	2	177	30	49	20	0 %
199.2	(C13H26O)H+	CHO	1.5	2	134	21	46	21	0 %
205.09	(C12H12O3)H+	Ar-CHO	8.5	2	30	12	35	12	30 %
205.19	(C15H24)H+	Ar-CH	4	2	136	13	10	6	58 %

Table S5. n-Alkanes (C_8-C_{18}) measured by the GC-MS system in the gaseous exhaust emissions. The factors their measured intensity exceeded the calibration standard by are also shown for both fresh and aged exhaust gases. The highest point of calibration would correspond to EI of 18 mg kg_{fuel}^{-1}.

Compound	Exceedance of calibration	
	Fresh	Aged
n-Octane	x4	x2
n-Nonane	x5	x2
n-Decane	x8	x3
n-Undecane	x16	x4
n-Dodecane	x16	x4
n-Tridecane	x16	x4
n-Tetradecane	x16	x4
n-Pentadecane	x14	x3
n-Hexadecane	x14	x3
n-Heptadecane	x12	x2
n-Octadecane	x12	x2

References

Cappellin, L., Karl, T., Probst, M., Ismailova, O., Winkler, P. M., Soukoulis, C., Aprea, E., Märk, T. D., Gasperi, F., and Biasioli, F.: On quantitative determination of volatile organic compound concentrations using proton transfer reaction time-of-flight mass spectrometry. *Environmental Science and Technology*, *46*(4), 2283–2290. https://doi.org/10.1021/es203985t. 2012.

Hartikainen, A. H., Basnet, S., Yli-Pirilä, P., Ihalainen, M., Talvinen, S., Tissari, J., Mikkonen, S., Zimmermann, R., and Sippula, O.: Resolving emission factors and formation pathways of organic gaseous compounds from residential combustion of European brown coal. *Combustion and Flame*, *265*, 113485. https://doi.org/10.1016/j.combustflame.2024.113485. 2024.

Hartikainen, A., Tiitta, P., Ihalainen, M., Yli-Pirilä, P., Orasche, J., Czech, H., Kortelainen, M., Lamberg, H., Suhonen, H., Koponen, H., Hao, L., Zimmermann, R., Jokiniemi, J., Tissari, J., and Sippula, O.: Photochemical transformation of residential wood combustion emissions: Dependence of organic aerosol composition on OH exposure. *Atmospheric Chemistry and Physics*, *20*(11). https://doi.org/10.5194/acp-20-6357-2020. 2020.

Ihalainen, M., Tiitta, P., Czech, H., Yli-Pirilä, P., Hartikainen, A., Kortelainen, M., Tissari, J., Stengel, B., Sklorz, M., Suhonen, H., Lamberg, H., Leskinen, A., Kiendler-Scharr, A., Harndorf, H., Zimmermann, R., Jokiniemi, J., and Sippula, O.: A novel high-volume Photochemical Emission Aging flow tube Reactor (PEAR). *Aerosol Science and Technology*, *53*(3), 276–294. https://doi.org/10.1080/02786826.2018.1559918. 2019.

Mason, Y. C., Schoonraad, G.-L., Orasche, J., Bisig, C., Jakobi, G., Zimmermann, R., and Forbes, P. B. C.: Comparative sampling of gas phase volatile and semi-volatile organic fuel emissions from a combustion aerosol standard system. *Environmental Technology & Innovation*, *19*, 100945. https://doi.org/10.1016/j.eti.2020.100945. 2020.

Palm, B. B., Campuzano-Jost, P., Ortega, A. M., Day, D. A., Kaser, L., Jud, W., Karl, T., Hansel, A., Hunter, J. F., Cross, E. S., Kroll, J. H., Peng, Z., Brune, W. H., and Jimenez, J. L.: In situ secondary organic aerosol formation from ambient pine forest air using an oxidation flow reactor. *Atmospheric Chemistry and Physics*, *16*(5), 2943–2970. https://doi.org/10.5194/acp-16-2943-2016. 2016.